Presented at EUCASS 2017
Milan, ITALY

Modelling Powder Bed Additive Manufacturing Defects

H.W. Mindt, O. Desmaison and M. Megahed
ESI Group
Parc D'affaires Silic, 99 Rue Des Solets, 94513 Rungis Cedex, France

Abstract

The qualification of powder bed fusion processes is based on lengthy and expensive experimental trial and error. If models can be applied to predict process details and determine the probability of manufacturing defects, the qualification process could be accelerated and cost can be reduced significantly. This paper describes numerical results resolving powder bed fusion processes and defects that could potentially happen during manufacturing. A multi-physics and multiscale modelling platform is first introduced in section 1 before proceeding to present numerical results of several defects that have been observed experimentally.

1. Introduction

Powder bed fusion (PBF) process is a form of Additive Manufacturing (AM) that deposits very thin layers of metal (microns). A heat source melts the metallic powder in certain areas of the powder bed. These areas then solidify to become a section of the final build while the un-melted powder is removed at the end of the process. An additional powder layer is added, and the process is repeated. PBF therefore involves a wide range of length scales: The powder bed particles' diameter can range from 10 to 100 microns while the laser may need to travel several kilometres in due course of the material processing. The laser powder interaction takes a few micro seconds; while the build time can be several hours or days. Modelling all length and time scales is necessary to predict work piece material characteristics such as lack of fusion and boiling porosities, residual stresses and deformations. Attempting to pursue all physics aspects in one model is prohibitively expensive from a computational stand point; making it necessary to develop multi-scale models that exchange relevant information ensuring accurate predictions across all length and time scales.

To address the challenge of modelling additive manufacturing the problem is subdivided into 3 length scale categories: Micro-, macro and meso-length scales. The micro-model characterizes the melt pool with length scales ranging from a few microns to a few millimetres. The micro-model resolves powder scale processes and defects such as lack of fusion, boiling porosity and surface roughness. Macro models resolve the workpiece to analyse distortions during the manufacturing process providing important information about manufacturability. The final state of the workpiece including shape distortion and residual stresses are also predicted by macro models. Mesoscale models provide necessary material properties as needed [1, 2, 3, 4].

2. The Melting Process

During laser powder interaction, large amounts of energy are absorbed leading to powder melting and evaporation. The evaporation process leads to a recoil pressure that ejects liquid particles out of the melt pool [5]. Other phenomena also lead to ejection of liquid out of the melt pool such as powder bed non-uniformity and large thermal gradients in the melt pool. If the particles ejected are comparable in size to the powder being melted, they are not expected to pose a problem to the process. If the ejected particles are however much larger than the powder size distribution supplied, then it is expected that the process will encounter problems such as lack of fusion and/or interaction between the coater arm and the large particles leading to nonuniform powder bed or the build process crashing.

Figure 1 shows the stainless steel particle distribution after recoating of a previously processed layer. The powder spreading model was performed by the tools described in [2]. The now solidified lower layers of the build can be partially seen through the new powder layer. The coating direction is from left to right as depicted by the arrow. It can be readily seen that the solidified material acts like a dam during powder spreading. On the side, closest to the powder source, a high packing density is observed. On the opposite side, hardly any particles are deposited by the coating mechanism leading to a highly non-uniform powder bed.

Figure 2 shows a time sequence of images showing the melting of the newly spread powder layer. A single hatch of about 1 mm length is studied. The spot size is 80 µm, the laser power is 100 W and the scan speed is 1000 mm/s. The model takes energy irradiation and absorption into account, phase change, heat transfer and all three thermodynamic phases as well as temperature dependent surface tension. The melt pool analysis is performed using the models described in [1]; validation examples can be found in [6, 7].

The molten surface can be easily identified by its wavy shape and the high temperatures of the processed material. The maximum temperature corresponds to the boiling temperature leading to metal evaporation. During the process, particles are ejected at relatively high speeds. If the particles are comparable in size with the powder particles being processes, they are extracted by the solver to retain largest possible time step sizes. Near a geometric instability of the previous layer, large amounts of the melt are ejected leading to a depression in the melt pool surface that is not recovered. The large particle ejected from the melt pool lands on the processing table leading to processing defects that are discussed in the following sections.

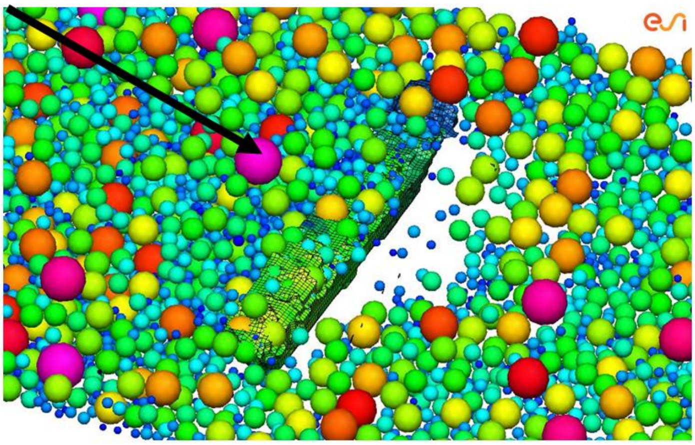

Figure 1: Recoated powder distributed on a previously processed layer showing nonuniformities of the new powder bed due to powder particle interaction with the build.

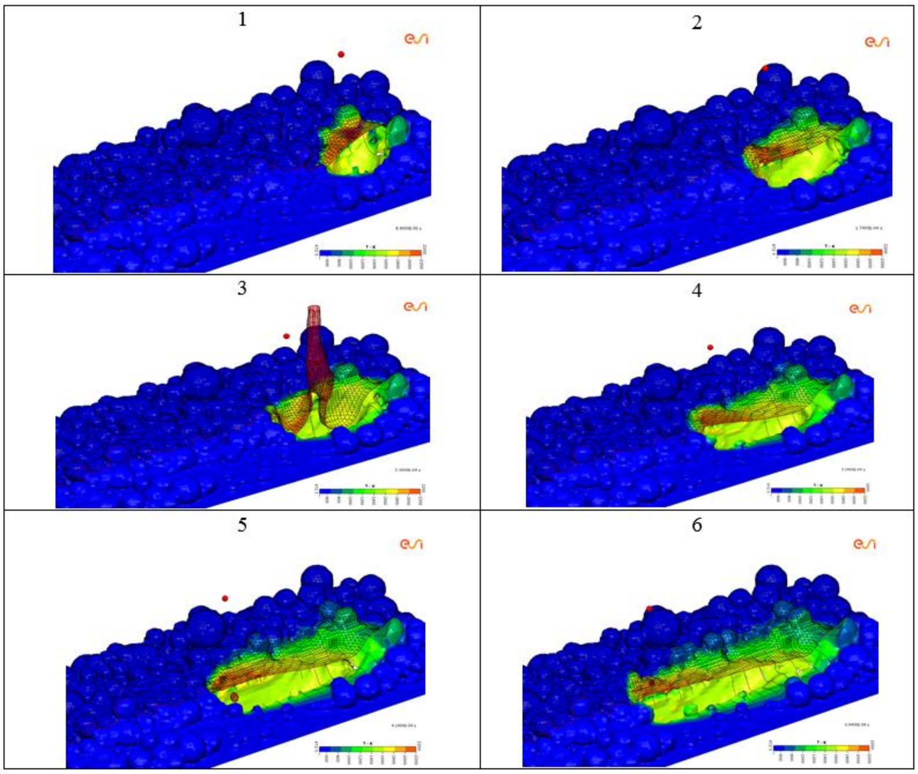

Figure 2: Melt pool evolution during processing of a newly spread layer – Sequence shows ejection of large particles.

4. Particle dragging – Non-uniform powder bed

When recoating the now processed material (3rd layer to be discussed), the powder was foreseen to have a large particle representative of the spatter volume discussed in the previous section. Figure 3 shows how this large particle pushed ahead of the rigid coater arm creating a line through the new powder bed where no particles are deposited.

The result is a nonuniform powder bed, that may lead to several subsequent issues like, high surface roughness that might lead to further nonuniformities of the next layer. Nonuniform layer thicknesses may lead to excessive layer thickness leading to lack of fusion defects or, as discussed in section 3, to large splatter.

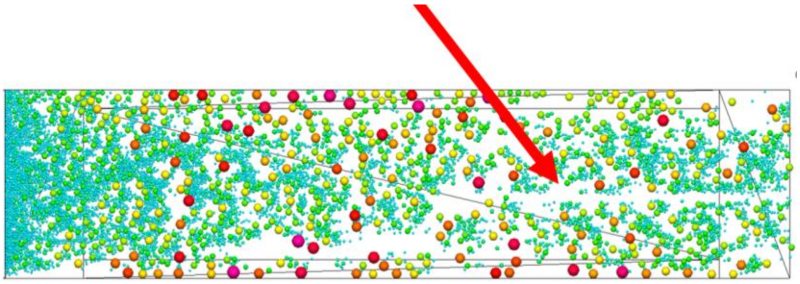

Figure 3: Non-uniform powder spreading to the dragging of large splatter particles.

5. Porosity

Powder bed fusion processes are prone to porosity. In all parameter studies performed the porosity was linked to enclosing of gas in the molten liquid as shown in Figure 4. During solidification two time scales become important: The time needed for the bubble to float out of the melt and the time required for the melt to solidify.

The gas pores originate from the gas available in the build chamber and exists between the powder particles and/or from keyholing phenomena where the metal evaporates and vapor is trapped in the deep melt pool. The small sized bubbles are usually strongly affected by melt pool flow conditions and do not have a strong buoyancy force, implying that the rapid solidification usually dominates.

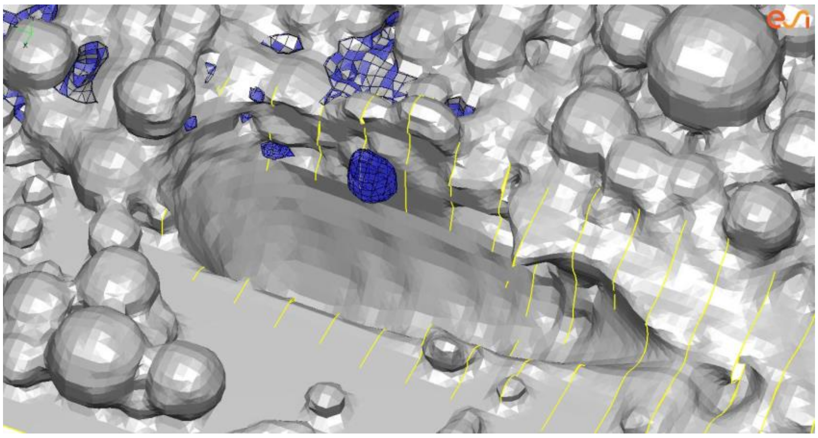

Figure 4: Top view of the melt pool, where the upper surface is hidden. The melt pool shape and dimensions can be readily measured. The blue sphere shows a bubble that was captured in the melt pool and that is later captured on the solidifying material.

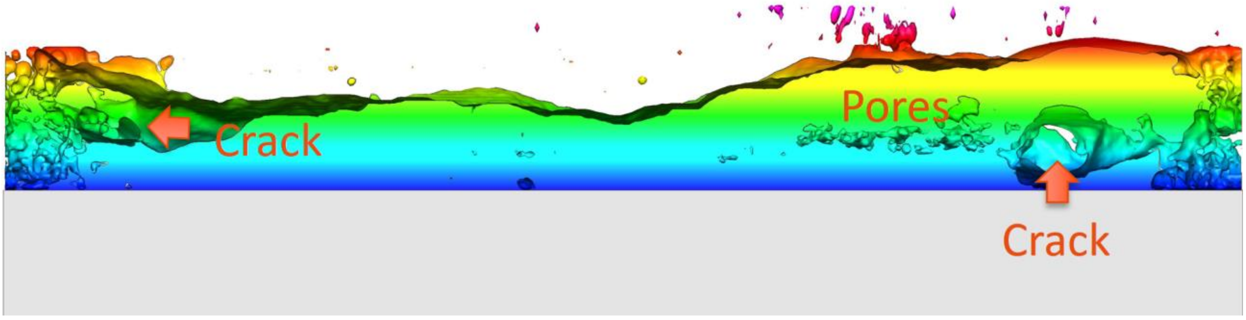

Figure 5: Side view of processed material showing the quality of the consolidated material. The numerical results show porosities and cracks that will affect the final product strength negatively.

The nonuniform powder bed resulting from previous imperfections is studied to investigate the affect the final product quality (Figure 5). The processing parameters choses were finetuned for a certain powder layer thickness corresponding to the central part of the domain. This leads to optimal consolidation of the powder. The thicker edges of this build however show how the increased amount of powder leads to higher concentrations of pores and cracks that will impact the final product strength.

6. Workpiece Distortion

The energy deposited into the material used during additive manufacturing processes leads to distortions and residual stresses that may impact the process and the final workpiece shape negatively. The vertical distortion of single layers can be comparable with the powder layer thickness. If the distortion is larger than the gap between the coater arm and the upper surface of the workpiece, the build process might be terminated due to too strong interaction between build and coater arm. If the distortion during the build process is managed correctly, that the build process is successfully finalized, residual stresses and workpiece distortions might lead to the component deviating too strongly from the intended design and/or shape. The ability of numerical models to predict both large-scale defects is demonstrated in the next section.

The manufacturability analysis is carried out for a Dome geometry presented in the Figure 6. Two different setups are considered, the first one (Case 1) considering the supported surface A only, the second one (Case 2) considering both supported surface A and B. The geometry is built in 140 successive layer depositions. The material is the Nickel Alloy Inconel 718®.

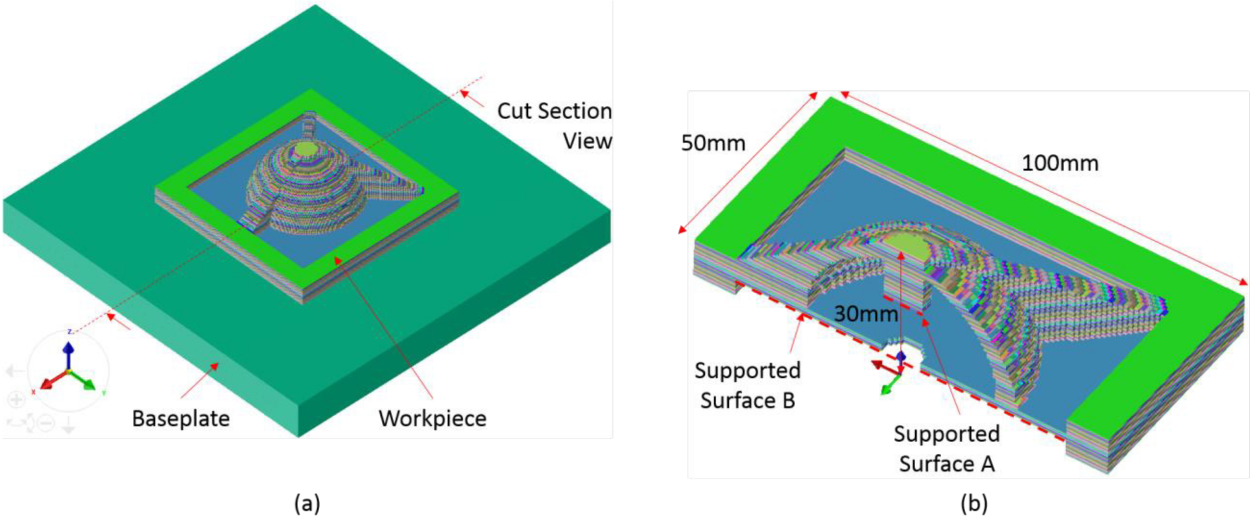

Figure 6: Dome Geometry: (a) 3D view with the baseplate, (b) Cut section view with supported surfaces.

The maximal vertical displacement of the last deposited layer is provided in Figure 7 (a) for the complete build. The corresponding main steps of build process are presented in the Figure 7 (b). By not supporting Surface B (Case 1), the risk of crashing the process is largely increased: the maximal vertical displacement of the build top from layer #17 (Step A) to layer #25 (Step B) is much higher than the table displacement. Nevertheless, the process seems to reduce this defect layer after layer and the distortion remains stable below the critical value. When the dome bell is almost achieved the risk increases again. During the building of the junction of the column above the supported surface A (both cases) and the dome bell (Step D), a decrease of the criterion is observed up to the end of the process.

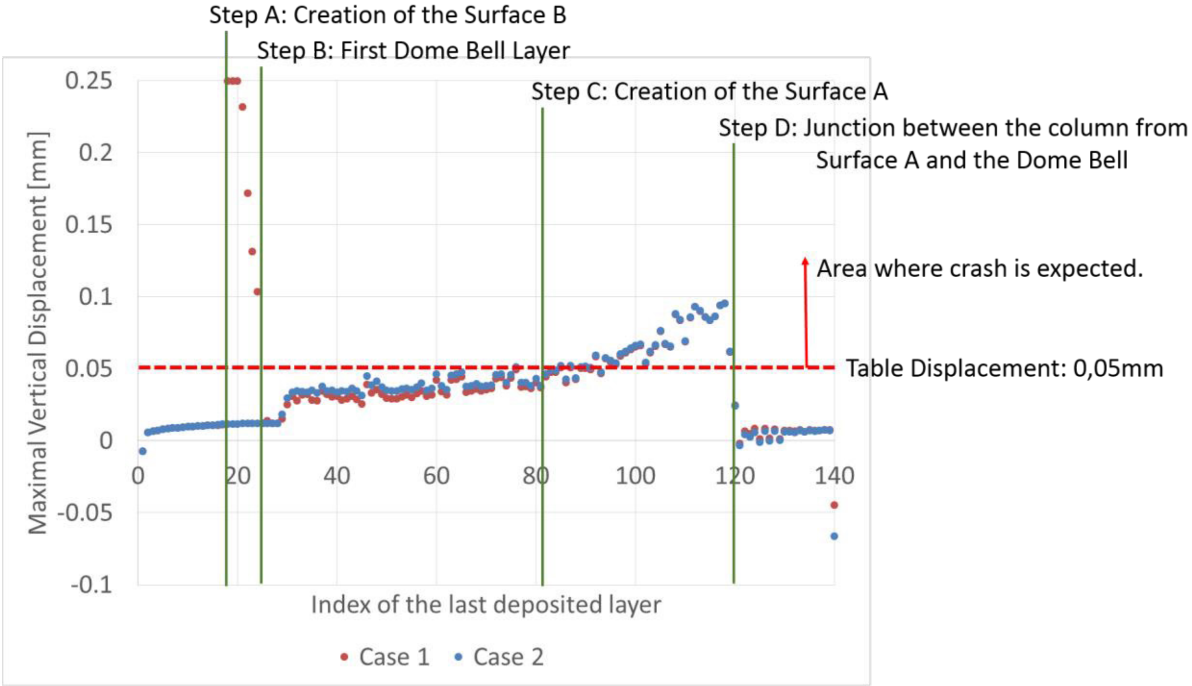

(a) Evolution of the maximal vertical displacement of the top layer during the building.

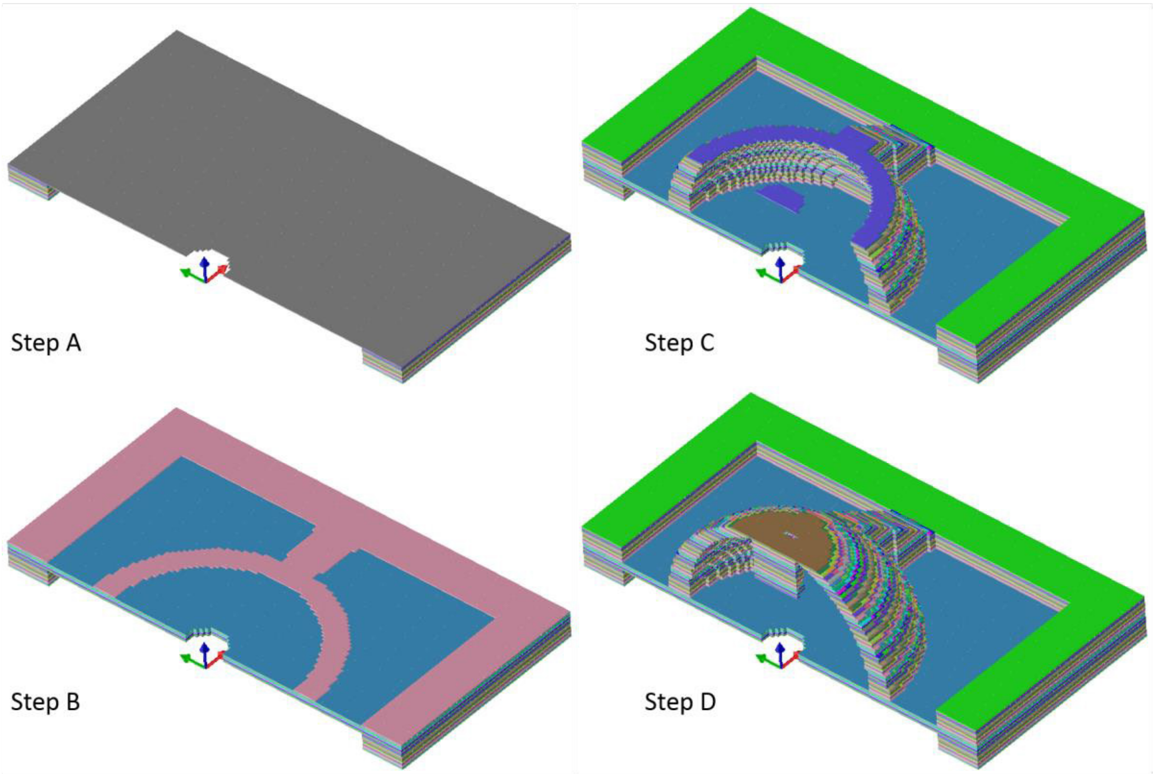

(b) Evolution of the building according to the graph steps.

Figure 7: Manufacturability Analysis.

Von Mises residual stresses and the vertical displacement distributions calculated after the removal of the workpiece from the baseplate is shown on the Figure 8 (Case 2 only). The base of the workpiece tends to bend while the stiffening walls constrain the distortion of the dome bell. The maximal residual stress distributions are located at the interface between the dome bell and the stiffening walls.

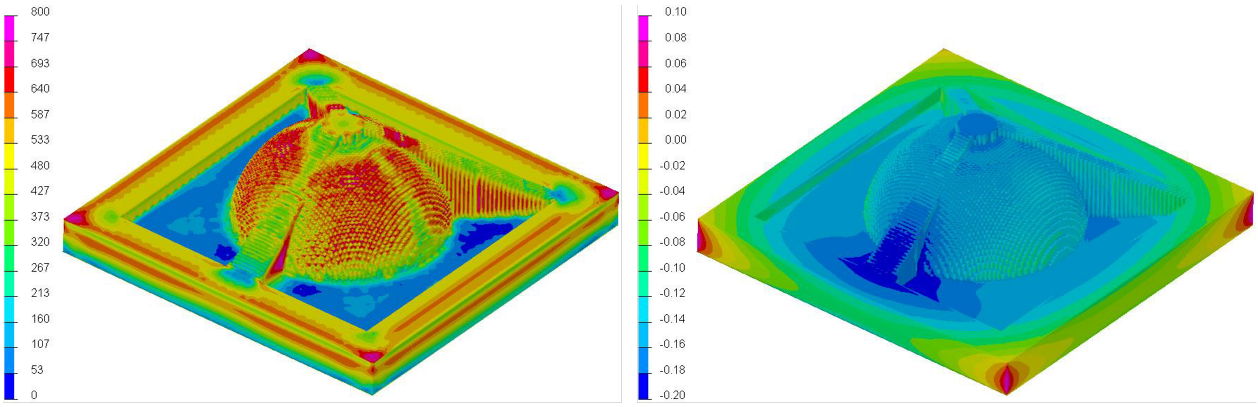

(a) Von Mises Residual Stress[MPa] (b) Vertical Displacement [mm]

Figure 8: Variable distributions after removal of the workpiece from the baseplate for the Case 2.

5. Summary & Conclusions

A Multiphysics multi scale modelling platform was demonstrated to capture powder scale and workpiece scale defects. Powder layer non-uniformities lead to large splatter particles being ejected out of the melt pool. These large particles in their turn cause non-uniformities in new powder layers. Processing parameters cannot always deliver densities above 99%. In many cases, where the powder size distribution, powder layer thickness and/or uniformity or splatter sizes are not favourable, gas bubbles are captured on the solidifying material.

The thermal input used to create the work piece leads to residual stresses and distortions at workpiece level. Numerical models were shown to predict manufacturability as well as the final component shape.

References

1. Megahed M, Mindt HW, N'Dri N, Duan HZ, Desmaison O (2016) Metal Additive Manufacturing Process and Residual Stress Modelling. Integrating Materials and Manufacturing Innovation. doi:10.1186/s40192-016-0047-2.
2. Mindt HW, Megahed M, Lavery NP, Holmes MA, Brown SGR (2016) Powder bed layer charateristics: The overseen first-order process input. Metallurgical and Materials Transactions A. 47(8) doi:10.1007/s11661-016-3470-2.
3. Peralta AD, Enright M, Megahed M, Gong J, Roybal M, Craig J (2016) Towards rapid qualification of powder-bed laser additively manufactured parts. Integrating Materials and Manufacturing Innovation. doi:10.1186/s40192-016-0052-5.
4. Desmaison O, Pires PA, Levesque G, Peralta A, Sundarraj S, Makinde A, et al. (May 21-25, 2017) Influence of computational grid and deposit volume on residual stress and distortion prediction accuracy for additive manufacturing modeling. 4th World congress on integrated computational materials engineering - ICME 2017, Ypsilanti, Mi, USA.
5. King WE, Anderson AT, Ferencz RM, Hodge NE, Kamath C, Khairallah SA, et al. (2015) Laser powder bed fusion additive manufacturing of metals; physics, computational, and materials challenges. Applied Physics Reviews. 2(041304) doi:10.1063/1.4937809.
6. H.-W. Mindt, Brian Shula, M. Megahed, A. D. Peralta, J. Neumann, Powder Bed Models – Numerical Assessment of As-Built Quality, AIAA 2016-1657, AIAA Science and Technology Forum and Exposition 2016, 4-8 January, 2016, San Diego, CA, USA. DOI: 10.2514/6.2016-1657.
7. J. Zielinski, H.-W. Mindt, M. Megahed, Influence of Powder Bed Characteristics on Material Quality in Additive Manufacturing, Metal Additive Manufacturing Conference, Nov. 24-28, 2016, Linz, Austria.